Complex magnetic phase diagram of ferromagnetic $CeNiSb_3$

V. A. Sidorov,[1,*] E. D. Bauer,[1] H. Lee,[2] S. Nakatsuji,[3] J. D. Thompson,[1] and Z. Fisk[2,†]
[1]*Los Alamos National Laboratory, Los Alamos, New Mexico 87545, USA*
[2]*Department of Physics, University of California, Davis, California 95616, USA*
[3]*Department of Physics, Graduate School of Science, Kyoto University, Kyoto 606-8502, Japan*
(Received 8 October 2004; revised manuscript received 2 December 2004; published 25 March 2005)

Measurements of electrical resistivity at applied pressures up to 55 kbar have been carried out on single crystals of the ferromagnet $CeNiSb_3$ revealing a complex magnetic phase diagram. The ferromagnetism at ambient pressure at $T_c=6$ K first increases with pressure up to 25 kbar, then decreases slightly for $P>25$ kbar. In the pressure range 35 kbar$\leqslant P\leqslant$55 kbar, a second anomaly in the resistivity is found at T_{M2}, below another higher temperature magnetic phase that is conjectured to be different than the ferromagnetism present at lower pressure. Changes in the physical properties such as the residual resistivity, and low temperature maximum in $\rho_{mag}(T)$ suggest a modification of the electronic structure where the two magnetic phases coexist with one another above 35 kbar. The critical pressure for the suppression of the lower temperature phase is estimated to be $P_c^{mag2}\simeq 55$ kbar, while the increase of both the T^2 coefficient of the electrical resistivity A and residual resistivity ρ_0 is suggestive of a quantum critical point associated with the higher temperature magnetic phase at $P_c^{mag1}\sim 60$ kbar.

DOI: 10.1103/PhysRevB.71.094422 PACS number(s): 71.27.+a, 72.15.Qm, 91.60.Gf

The occurrence of exotic ground states in the vicinity to a second-order phase transition tuned to zero temperature, or quantum critical point (QCP), has attracted considerable attention in recent years. Pressure tuning of antiferromagnetic f-electron heavy-fermion compounds has been particularly fruitful in uncovering these emergent ordered phases near the quantum critical point as well as elucidating the unusual power law or logarithmic temperature dependences of the physical properties, or non-Fermi liquid (NFL) behavior, arising from the abundant quantum fluctuations in the vicinity of the QCP (for a recent review, see Ref. 1). For instance, a dome of superconductivity with $T_c^{max}\sim 0.4$ K in $CePd_2Si_2$ is found near an antiferromagnetic instability at a critical pressure $P_c=28$ kbar.[2] At P_c, the normal state electrical resistivity is best described by a NFL power law T dependence $\rho-\rho_0=AT^n$ with $n=1.2$ in contrast to the T^2 behavior expected for a Fermi liquid. More recently, forms of order have been observed near a ferromagnetic (FM) QCP, such as the coexistence of superconductivity and FM order in UGe_2,[3] a non-Fermi liquid ground state in the presence of ferromagnetism,[4] or the occurrence of a magnetic phase near the FM QCP in $CeAgSb_2$.[5] It is therefore of interest to investigate f-electron systems near a ferromagnetic instability. To this end, we present measurements of electrical resistivity up to 55 kbar on ferromagnetic $CeNiSb_3$.

$CeNiSb_3$ adopts the orthorhombic *Pbcm* structure comprised of alternating Ce, Ni-centered octahedra, buckled planar Sb layers.[6] It is one of the few Ce-based compounds to order ferromagnetically ($T_c=6$ K). Magnetization measurements[7] indicate large magnetocrystalline anisotropy with an easy axis saturation magnetization $M_{sat}^c=1.55\ \mu_B$/Ce atom along the c direction, $M_{sat}^b=0.95\ \mu_B$/Ce atom, and a hard axis with $M_{sat}^a(6\text{ T})=0.12\ \mu_B$/Ce atom along the a direction. Curie-Weiss fits to the magnetic susceptibility data yield an average effective moment $\mu_{eff}=2.58\ \mu_B$, close to that expected for trivalent Ce ($\mu_{eff}=2.54\ \mu_B$); the Curie-Weiss temperatures reveal strong ferromagnetic correlations along the c axis ($\theta_{CW}^c=29$ K) and antiferromagnetic correlations in the ab plane ($\theta_{CW}^a=-156$ K). Bulk ferromagnetism is confirmed by the large anomaly in the specific heat. Both the small value of the Sommerfeld coefficient $\gamma\sim 50$ mJ/mol K^2 and magnetic entropy released below the transition $S_{mag}\simeq 4.4$ J/mol K$=(0.75)Rln(2)$ indicate a modest Kondo interaction within a crystal-field (CF) split doublet ground state of Ce in $CeNiSb_3$. At high temperatures, a Schottky-like anomaly at $\sim$70 K in the magnetic specific heat indicates excitations to an excited CF level; the magnetic entropy up to 300 K $S_{mag}(300\text{ K})\simeq 14$ J/mol K is very close to the entropy expected for the full Ce $J=5/2$ Hund's rule multiplet $Rln(6)=14.9$ J/mol K.

Single crystals of $CeNiSb_3$ were grown in excess Sb flux.[8] The orthorhombic *Pbcm* structure was confirmed by powder x-ray diffraction.[6] Electrical resistivity measurements under pressure were carried out using both a Be/Cu piston-cylinder clamped device and a profiled toroidal anvil clamped device[9] with anvils supplied with a boron-epoxy gasket and Teflon capsule, containing pressure-transmitting liquid, sample, and a pressure sensor. The pressure was determined from the variation of the superconducting transition of lead using the pressure scale of Eiling and Schilling.[10] The width of the Pb transition implied a pressure gradient of $\lesssim$0.5 kbar at the highest pressure. A standard four-probe technique was performed using an LR-700 Linear Research bridge operating at a current of 1 mA applied along the b axis of the crystal.

The electrical resistivity $\rho(T)$ of $CeNiSb_3$ at various applied pressures is displayed in Fig. 1. At ambient pressure, the resistivity is weakly temperature dependent above 150 K and reaches a minimum at $\sim$30 K followed by a maximum at $\sim$20 K, before decreasing rapidly in the ferromagnetic state. Upon subtraction of the nonmagnetic contribution of $LaNiSb_3$, the magnetic scattering $\rho_{mag}\equiv\rho(CeNiSb_3)-\rho(LaNiSb_3)$ exhibits a logarithmic temperature dependence

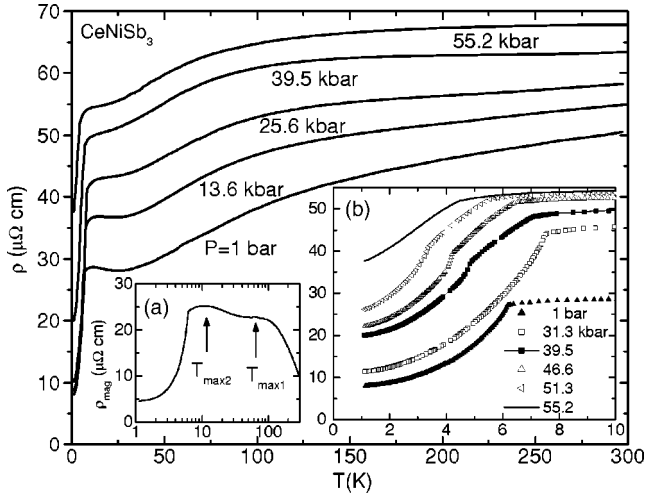

FIG. 1. Electrical resistivity $\rho(T)$ of $CeNiSb_3$ at various pressures P. Inset (a) Magnetic contribution of the electrical resistivity ρ_{mag} at ambient pressure. The arrows indicate the temperature of the shoulder (or maximum) T_{max1} and low-T maximum T_{max2} in ρ. Inset (b) $\rho(P,T)$ below 10 K.

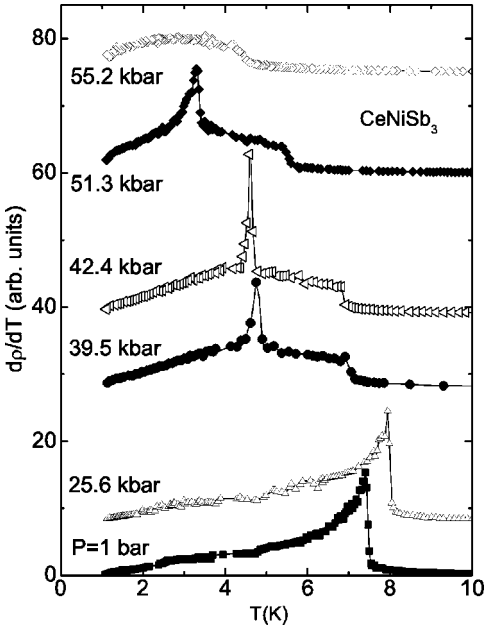

FIG. 2. $d\rho/dT$ vs T at various pressures of $CeNiSb_3$. The curves have been offset for clarity.

above ~200 K, characteristic of Kondo systems, and two broad maxima (or shoulder) at $T_{max1} \sim 77$ K and $T_{max2} = 10.8$ K s shown in inset (a) of Fig. 1. The low-T maximum in $\rho(T)$ is assumed to be related to the Kondo lattice coherence,[11] while the high temperature maximum at T_{max1} is associated with scattering from an excited crystal field level, consistent with the Schottky anomaly observed in specific heat measurements. Below 10 K, the ferromagnetic transition temperature first increases with applied pressure up to 31.3 kbar, then begins to decrease at higher pressure up to 35.6 kbar. At $P = 39.5$ kbar, a sharp kink in $\rho(T)$ at $T_{M2} = 5$ K signals the onset of a second phase transition below the upper one at $T_{M1} = 7$ K. The change in slope of $\rho(T)$ in between the two transitions for $P \geqslant 39.5$ kbar, suggests that the ferromagnetic phase transforms into a phase that is coexistent with the lower temperature phase. Both magnetic transitions are observed between 39.5 and 51.3 kbar and decrease with increasing pressure up to $P = 55.2$ kbar, at which point only the upper transition is found.

The evolution of the magnetic phase transitions of $CeNiSb_3$ with pressure is clearly illustrated by anomalies in the first derivative $d\rho/dT$ as shown in Fig. 2. If the relation between specific heat and $d\rho/dT$ is assumed to hold,[12] the ferromagnetic transition appears to be second-order up to 31.3 kbar, where the shape of the anomaly associated with this transition then changes at $P = 39.5$ kbar. The lower transition at T_{M2} is sharp and first-order-like up to 42.4 kbar, but then attains a broader shape more characteristic of a second-order phase transition at $P = 51.3$ kbar; for $P > 51.3$ kbar, only an anomaly associated with the upper transition at T_{M1} is observed.

Figure 3 shows the low temperature power law fits ($\rho - \rho_0 = AT^n$) to the $\rho(P,T)$ data of $CeNiSb_3$. The exponent n is about 3 up to the maximum in the Curie temperature at 25 kbar and exhibits a local minimum close to the pressure where there is coexistence of two magnetic phases in the range 35.6 kbar $\leqslant P \lesssim$ 55 kbar. Fermi liquid behavior is recovered at pressures of 51.3 and 55.2 kbar. The generalized A coefficient of the power law fits increases by an order of magnitude between ambient pressure and $P = 55.2$ kbar; at this pressure, the empirical Kadowaki-Woods relation[13] $[A/\gamma^2 = 1 \times 10^{-5}\ \mu\Omega\ \text{cm (mol K/mJ)}^2]$ implies a heavy Fermi liquid ground state with $\gamma \sim 300$ mJ/mol K.[2] Fits of the data to activated behavior associated with a gap in the magnon dispersion[5] proved unsatisfactory for all pressures and only the data at the highest pressures of 51.3 and 55.2 kbar could be fit to a T^2 contribution [in agreement with the power law fits shown in Fig. 3(b)].

Figure 4 provides a summary of our electrical resistivity measurements under pressure on $CeNiSb_3$. At modest pressures, the Curie temperature first increases with increasing pressure, then decreases, passing through a maximum at 25 kbar. Features in the various physical properties [the abrupt jump in ρ_0, change in slope of $A(P)$, etc.] signal the onset of a second (lower) phase at T_{M2} at ~35 kbar. For 40 kbar $\leqslant P \lesssim$ 55 kbar, there is evidence for two phase transitions in the $\rho(P,T)$ curves, which we postulate are magnetic in nature and different from the ferromagnetism present at lower pressure. It is likely that one or both of these phases are antiferromagnetic since $PrNiSb_3$ exhibits antiferromagnetic order at $T_N = 4.5$ K and has a similar unit cell volume to that of $CeNiSb_3$ under pressure.[14] The increase of A and ρ_0 at the highest pressures is suggestive of a quantum critical point at $P_c^{mag1} \sim 60$ kbar associated with the suppression of the upper magnetic phase at T_{M1}.

There is growing evidence that the $CeTSb_3$ and $CeTSb_2$ ferromagnets are unstable to new forms of magnetic order. In $CeNiSb_3$, the change in shape of the $\rho(T)$ curves for $P \geqslant 40$ kbar and the presence of a second magnetic phase at T_{M2} suggests the emergence of a new phase at T_{M1} descendent from the ferromagnetism at lower pressure. The appear-

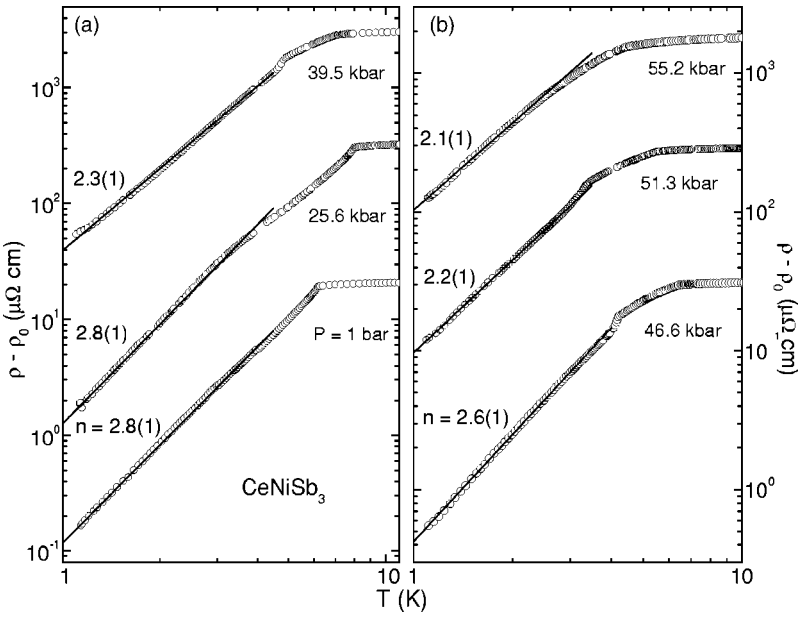

FIG. 3. (a) $\rho-\rho_0$ vs T for $P\leqslant 39.5$ kbar on a log-log scale of $CeNiSb_3$. Each of the curves have been shifted vertically by one decade from the curve below it for clarity. (b) $\rho-\rho_0$ vs T for 46.6 kbar$\leqslant P\leqslant$55.2 kbar. The lines in (a) and (b) are power law fits to the data yielding the exponent n indicated beside each curve where the uncertainty in the last digit is indicated by the number in the parentheses. The deviations from the power law behavior at $\sim$4 K of the data at 1 bar and 25.6 kbar are an experimental artifact.

ance (or disappearance) of these two phases seems not to be related to a change in the crystal field ground state as the feature at T_{max1} decreases only slightly upon the application of 60 kbar. In addition, the smooth evolution of the coherence feature at T_{max2} indicates the occurrence of the new phases are not associated with a drastic change in the electronic structure. A complex magnetic T-P phase diagram is also revealed in the heavy-fermion ferromagnet $CeAgSb_2$.[5]

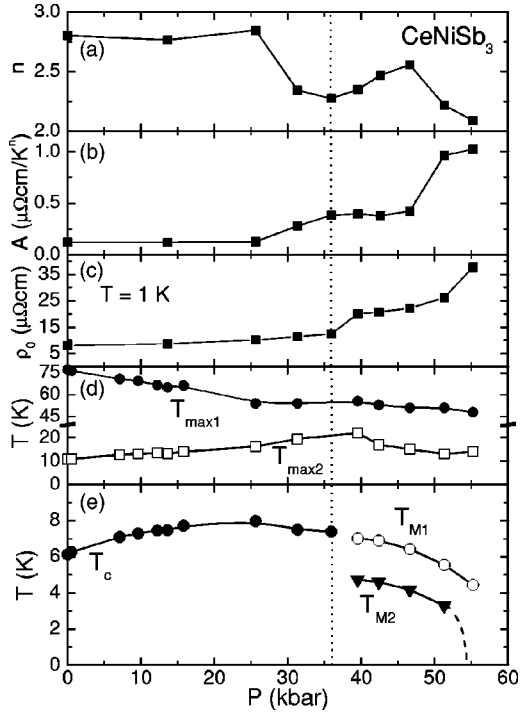

FIG. 4. Power law exponent n, coefficient A, residual resistivity ρ_0, features in the magnetic contribution to the resistivity T_{max1} and T_{max2}, and magnetic ordering temperatures T_c, T_{M1}, T_{M2} vs P in (a)–(d), respectively. The lines are guides to the eye.

In this material, ferromagnetism at $T_c=10$ K at $P=0$ kbar is suppressed at $P_c=35$ kbar. In a narrow pressure range ($\sim$5 kbar) below P_c, a first order transition occurs between a (presumed) antiferromagnetic state ($T_N\sim 5$ K) and the ferromagnetic phase. A sharp maximum in the A coefficient of the T^2 behavior and also ρ_0 at P_c is the only evidence of quantum criticality; any low-T NFL behavior is likely obscured by the antiferromagnetism at $T_N\sim 2-4$ K in this pressure range. In contrast to $CeNiSb_3$, a distinct feature in the low-T maximum in the $\rho(T)$ curves at T_{max} is found close to P_c in $CeAgSb_2$. Preliminary measurements on $CeZnSb_2$ indicate ferromagnetism at $T_C\sim 6$ K coexisting with a spin glass phase at lower temperature up to 60 kbar.[15] The unusual magnetic phase diagrams of all three of the Ce-based ferromagnets indicate the competition between the Ruderman-Kittel-Kasuya-Yosida (RKKY) interaction, which promotes magnetic order, and the Kondo effect, which suppresses magnetic order, is more complex than originally proposed by Doniach[16] and is influenced by such factors as magnetocrystalline anisotropy and crystal field effects.

In summary, measurements of electrical resistivity under pressure on $CeNiSb_3$ reveal a complex magnetic phase diagram. Ferromagnetism in this material is only slightly suppressed for $P>35$ kbar before a second phase transition is found at T_{M2} below another higher temperature magnetic phase. Changes in the physical properties such as the residual resistivity, and coherence maximum in $\rho_{mag}(T)$ suggest a modification of the electronic structure upon entering this two phase region above 35 kbar. The critical pressure for the suppression of the lower temperature phase is estimated to be $P_c^{mag2}\simeq 55$ kbar, while the increase of both the T^2 coefficient of the electrical resistivity A and residual resistivity ρ_0 is suggestive of a quantum critical point associated with the higher temperature magnetic phase at $P_c^{mag1}\sim 60$ kbar.

Work at Los Alamos was performed under the auspices of the U.S. DOE. V.A.S. acknowledges the support of Russian

Foundation for Basic Research Grant No. 03-02-17119 and Programs "Strongly Correlated Electrons" and "High Pressures" of the Department of Physical Sciences, Russian Academy of Sciences. Research at UC-Davis was supported by the NSF under Grant No. NSF DMR 0433560. We thank Luis Balicas for assisting in the resistivity measurements under pressure at the NHMFL and Brad Carter for helping with the experiments.

*Also at: Institute for High Pressure Physics, Russian Academy of Sciences, 142190 Troitsk, Russia.

†Also at: Los Alamos National Laboratory, Los Alamos, NM 87545, USA.

[1] G. R. Stewart, Rev. Mod. Phys. **73**, 797 (2001).

[2] N. D. Mathur, F. M. Grosche, S. R. Julian, I. R. Walker, D. M. Freye, R. K. W. Haselwimmer, and G. G. Lonzarich, Nature (London) **394**, 39 (1998).

[3] S. S. Saxena, P. Agarwal, K. Ahllan, F. M. Grosche, R. K. W. Haselwimmer, M. J. Steiner, E. Pugh, I. R. Walker, S. R. Julian, P. Monthoux, G. G. Lonzarich, A. Huxley, I. Sheikin, D. Braithwaite, and J. Flouquet, Nature (London) **406**, 587 (2000).

[4] E. D. Bauer, V. S. Zapf, P.-C. Ho, N. P. Butch, E. J. Freeman, C. S. Sirvent, and M. B. Maple, Phys. Rev. Lett. **94**, 046401 (2005).

[5] V. A. Sidorov, E. D. Bauer, N. A. Frederick, J. R. Jeffries, S. Nakatsuji, N. O. Moreno, J. D. Thompson, M. B. Maple, and Z. Fisk, Phys. Rev. B **67**, 224419 (2003).

[6] R. T. Macaluso, D. M. Wells, R. E. Sykora, T. E. Albrecht-Schmitt, A. Mar, S. Nakatsuji, H. Lee, Z. Fisk, and J. Y. Chan, J. Solid State Chem. **177**, 293 (2004).

[7] H. Lee, S. Nakatsuji, Y. Chen, W. Bao, M. F. Hundley, R. T. Macaluso, J. Y. Chan, B. Carter, P. Klavins, P. Schlottmann, and Z. Fisk (unpublished).

[8] Z. Fisk and J. P. Remeika, in *Handbook on the Physics and Chemistry of the Rare Earths*, edited by K. A. Gschneidner, Jr. and L. Eyring (North-Holland, Amsterdam, 1989), Vol. 12, Chap. 81, p. 53.

[9] L. G. Khvostantsev, V. A. Sidorov, and O. B. Tsiok, in *Properties of Earth and Planetary Materials at High Pressures and Temperatures*, Geophysical Monograph 101, edited by M. H. Manghnani and T. Yagi (American Geophysical Union, Washington, DC, 1998), p. 89.

[10] A. Eiling and J. S. Schilling, J. Phys. F: Met. Phys. **11**, 623 (1981).

[11] J. D. Thompson and J. M. Lawrence, in *Handbook on the Physics and Chemistry of the Rare Earths*, edited by K. A. Gschneidner, Jr., L. Eyring, G. H. Lander, and G. R. Choppin (North-Holland, Amsterdam, 1994), Vol. 19, Chap. 133, p. 383.

[12] M. E. Fisher and J. S. Langer, Phys. Rev. Lett. **20**, 665 (1968).

[13] K. Kadowaki and S. B. Woods, Solid State Commun. **58**, 307 (1986).

[14] E. L. Thomas, R. T. Macaluso, H. Lee, Z. Fisk, and J. Y. Chan, J. Solid State Chem. **177**, 4228 (2004).

[15] T. Park, V. A. Sidorov, J. D. Thompson, H. Lee, and Z. Fisk (unpublished).

[16] S. Doniach, Physica B **91**, 231 (1977).